

# Searching for gravitational waves from compact binary mergers powering long gamma-ray bursts during LIGO-Virgo-KAGRA's O3 run

MALLIKA R. SINHA,<sup>1, 2</sup> TEAGAN A. CLARKE,<sup>3, 1, 2</sup> QIFANG ZHANG,<sup>1, 2</sup> NIKHIL SARIN,<sup>4, 5</sup> ERIC THRANE,<sup>1, 2</sup> AND PAUL D. LASKY<sup>1, 2</sup>

<sup>1</sup>*School of Physics and Astronomy, Monash University, Clayton VIC 3800, Australia*

<sup>2</sup>*OzGrav: The ARC Centre of Excellence for Gravitational Wave Discovery, Clayton VIC 3800, Australia*

<sup>3</sup>*Department of Physics, Princeton University, Princeton, New Jersey, 08544, USA*

<sup>4</sup>*Kavli Institute for Cosmology, University of Cambridge, Madingley Road, CB3 0HA, UK*

<sup>5</sup>*Institute of Astronomy, University of Cambridge, Madingley Road, CB3 0HA, UK*

## ABSTRACT

Neutron star binary mergers are often associated with short gamma-ray bursts (GRBs), but the recent detection of kilonovae coincident with long GRBs suggest that some mergers may produce long GRBs. Motivated by these developments, we perform a search for binary neutron star and neutron star-black hole gravitational-wave signals coincident with long GRBs using data from the third LIGO–Virgo–KAGRA (LVK) observing run. We analyze LVK data coincident with long GRBs detected by Fermi’s GRB Monitor and Swift’s Burst Alert Telescope when at least two gravitational-wave observatories were running. We find no evidence of a coincident gravitational-wave signal and set limits on the luminosity distance to each of these long GRBs under the assumption that they were powered by binary mergers.

## 1. INTRODUCTION

Gamma-ray bursts (GRBs) are extremely energetic emissions of gamma rays that can last anywhere from milliseconds to hours (e.g., Zhang 2018; Neights et al. 2025). The progenitors of GRBs have been debated since their discovery. Bimodality in their temporal and spectral properties has given rise to the classification of short-hard ( $< 2$  s) and long-soft ( $> 2$  s) GRBs (Kouveliotou et al. 1993). The former are thought to be produced by mergers of a neutron star with another neutron star or stellar-mass black hole (Paczynski 1991; Eichler et al. 1989; Popham et al. 1999; Narayan et al. 1992) (supported by the coincident GRB and gravitational-wave detection of GW170817 and GRB170817A (Abbott et al. 2017a,b; Savchenko et al. 2017; Goldstein et al. 2017)), and the latter from the core collapse of massive stars (Woosley 1993; Paczyński 1998; Popham et al. 1999).

Recent observations of three long GRBs casts doubt on the above classification, with evidence their progenitors were compact binary mergers involving at least one neutron star. Optical/infrared kilonovae signals

have been associated with GRBs GRB060614 (Gehrels et al. 2006; Della Valle et al. 2006; Zhang et al. 2007; Jin et al. 2015), GRB211211A (Rastinejad et al. 2022; Troja et al. 2022; Yang et al. 2022; Zhang et al. 2022) and GRB230307A (Yi et al. 2025; Levan et al. 2023; Sun et al. 2024; Yang et al. 2023; Maccary et al. 2026; Gillanders & Smartt 2025), suggesting the duration of GRBs may not uniquely map to the type of progenitor.<sup>1</sup> Whereas the first two of these three long GRBs show tentative kilonova associations based on their temporal lags and spectral properties, GRB230307A shows a slightly stronger connection, marked by tellurium emission lines indicative of active  $r$ -process nucleosynthesis.

Given the limited understanding of the exact physical processes governing the creation of GRBs, it remains unclear how properties other than the progenitor may determine the classification of GRBs. There are theoretical frameworks that support compact binary merger powered long GRBs (e.g., Gottlieb et al. 2023; Rosswog et al. 2024). Thus far, no type of gravitational-wave sig-

<sup>1</sup> Some suggested influential factors other than the progenitor include energy dissipation processes, environmental factors, disk mass, and the emission mechanism (e.g., Yi et al. 2025; Gottlieb et al. 2023; Gompertz et al. 2022; Zhu et al. 2025; Maccary et al. 2026).

nal has been confidently observed coincident with a long GRB (Abbott et al. 2021, 2022; Wang et al. 2022; Abbott et al. 2019b; Aasi 2014; Abbott 2017). A coincident long GRB–gravitational-wave merger detection would provide unambiguous evidence linking at least some long GRBs to binary mergers. We perform a modelled search for sub-threshold binary neutron star and neutron star–black hole merger gravitational-wave signals in data from the third observing run of the LIGO (Aasi et al. 2015), Virgo (Acernese et al. 2014), KAGRA (Akutsu et al. 2020) (LVK) network (Abbott et al. 2023b).<sup>2</sup> We look for mergers coincident with long GRBs detected by Fermi’s GRB Monitor (GBM; Meegan et al. 2009), and Swift’s Burst Alert Telescope (BAT; Gehrels et al. 2004; Barthelmy et al. 2005; Tohuvavohu et al. 2020).

The structure of the Paper is as follows. In Sec. 2, we outline our method and techniques used to perform the search. We then present the results of our analysis in Sec. 3, and conclude in Sec. 4.

## 2. METHODOLOGY

We use a subset of 70 long GRBs detected by Swift/BAT and Fermi/GBM that occurred during the third LVK observing run (Abbott et al. 2021, 2022) and had at the two LIGO gravitational-wave observatories running at the time. We obtain gravitational-wave data from the Gravitational-Wave Open Science Center (Abbott et al. 2023a). The set of GRBs and the observatories running at the time are listed in Table 3 in the Appendix. Each of these GRBs have been analysed before by the LVK Collaboration (Abbott et al. 2021, 2022), however those searches were for signals from collapsars, rather than neutron star coalescences. In other words, those LVK searches looked for coherent excess power between gravitational-wave observatories (Sutton et al. 2010; Was et al. 2012), rather than templated searches using binary neutron star and/or neutron star–black hole waveforms (e.g., Harry & Fairhurst 2011; Williamson et al. 2014; Sathyaprakash & Schutz 2009, Sec. 5).

We require LIGO Hanford (H) and LIGO Livingston (L) to be observing for a period of 1200 s without significant data quality issues around the GRB trigger time. We include Virgo (V) in our analysis if it was observing, but it is not a requirement. Of our 70 long GRBs, there are 48 with HLV data and 22 with HL data. There is no additional redshift or progenitor information for these long GRBs (Finneran et al. 2025).

<sup>2</sup> While Abbott et al. (2023b) defines sub-threshold signals as those with an inferred astrophysical compact binary merger probability below 50%, but a false alarm rate of less than two per day, we use the term more generally to mean signals that are not confidently detected.

For each long GRB, we perform parameter estimation and calculate the Bayesian evidence for a binary neutron star signal using the BILBY inference library (Ashton et al. 2019b; Romero-Shaw et al. 2020). We extract the Bayesian evidence from the nested sampling runs for individual detectors, and for a coherent analysis of the LVK network. For details of these calculations, we refer the reader to Sec. V of Abbott et al. (2023b). For most parameters we employ standard priors from Romero-Shaw et al. (2020). For the other parameters, we employ priors designed for our long GRB search; see Table 1.

We fix the sky location according to the electromagnetic trigger. We ignore the sky-location uncertainty from the electromagnetic trigger, which is small compared to the uncertainty in the sky location determined for an equivalent, sub-threshold, gravitational-wave event (Berlato et al. 2019; Barthelmy et al. 2005). Prompt GRB emission from a binary merger involving at least one neutron star is generally thought to be produced in a short window around the merger time,  $t_0$  (e.g., Zhang 2018). Following Abbott et al. (2021, 2022), we use the standard window  $t_0 = t_{\text{GRB}} + [-5, 1]$  s, where  $t_{\text{GRB}}$  is the GRB trigger time. This assumes the GRB trigger is created as some product of the merger, not from precursor or delayed prompt pulse emission. Our prior for luminosity distance  $D_L$  is uniform in comoving volume out to a maximum value of 2000 Mpc where we can be sure there is no chance of a gravitational-wave detection.<sup>3</sup>

We limit the progenitor masses  $m_1 \in [0.5, 6] M_\odot$  and  $m_2 \in [0.5, 2] M_\odot$  with  $m_1 \geq m_2$ . The upper limit on  $m_1$  is a conservative assumption that a system with a mass  $> 6M_\odot$  would not tidally disrupt the neutron star, and therefore not produce a long GRB (Shibata & Uryū 2006; Kyutoku et al. 2021). We do not limit the progenitor spins,  $\chi_1$  and  $\chi_2$  beyond the assumption the spins are aligned, and use a use prior on the magnitude of  $[0, 0.99]$ .

The waveforms are generated using the phenomenological IMRPHENOMD model for gravitational-wave signals with non-precessing spin (Husa et al. 2016; Khan et al. 2016). Waveforms with more underlying physics (such as tides or higher-order modes) exist and are used in GWTC-3 (Abbott et al. 2023b). However, since we

<sup>3</sup> The choice of maximum luminosity distance affects the value of the signal evidence. However, we interpret our signal evidence by comparing it with the distribution obtained from off-source data. (In essence, we are calculating a frequentist significance from a Bayesian evidence.) Since the off-source data is analyzed with the same prior, the statistical significance of a candidate event does not depend on the choice of prior boundary.

Parameter	Type	Range
$m_1$	uniform	$[0.5M_{\odot}, 6M_{\odot}]$
$m_2$	uniform	$[0.5M_{\odot}, 2M_{\odot}]$
$\chi_1$	uniform	$[0, 0.99]$
$\chi_2$	uniform	$[0, 0.99]$
$D_L$	uniform in comoving volume	$[50 \text{ Mpc}, 2000 \text{ Mpc}]$
RA	fixed	$\text{RA}_{\text{GRB}}$
Dec	fixed	$\text{DEC}_{\text{GRB}}$
$t_0$	uniform	$t_{\text{GRB}} + [-5 \text{ s}, +1 \text{ s}]$

**Table 1.** A summary of the priors used in our analysis. Here,  $m_i$  and  $\chi_i$  are the component masses and dimensionless spins,  $D_L$  is the luminosity distance, RA and Dec are the sky location, and  $t_0$  is the time of coalescence, where  $t_{\text{GRB}}$  is the GRB trigger time. For the other binary parameters we employ default priors from [Romero-Shaw et al. \(2020\)](#).

are searching for sub-threshold signals, we opt for fast waveforms, albeit with less precision than state-of-the-art alternatives.

We use the evidences to calculate the *Bayes coherence ratio* (BCR; [Veitch & Vecchio 2010](#); [Isi et al. 2018](#); [Ashton et al. 2019a](#); [Ashton & Thrane 2020](#)), which compares the “coherent evidence” (obtained using two or three observatories) to the “incoherent evidence,” which does not require consistency between observatories:

$$\text{BCR} = \frac{\mathcal{Z}_{\text{coherent}}}{\mathcal{Z}_{\text{incoherent}}}, \quad (1)$$

where

$$\mathcal{Z}_{\text{coherent}} \equiv \int d\theta \mathcal{L}(d_H, d_L, \dots | \theta) \pi(\theta), \quad (2)$$

and

$$\mathcal{Z}_{\text{incoherent}} \equiv \left( \int d\theta \mathcal{L}(d_H | \theta) \pi(\theta) \right) \times \left( \int d\theta' \mathcal{L}(d_L | \theta') \pi(\theta') \right) \dots, \quad (3)$$

where  $d_i$  are the data from the  $i$ th observatory.

Formally, the BCR is a Bayes factor comparing the hypothesis that there is an astrophysical signal in two or more detectors to the hypothesis that there are uncorrelated noise artefacts in both detectors that look like binary signals. True signals are consistent between observatories, which lead to large coherent evidences and hence large BCR values. Noise artefacts, on the other hand, can produce large signal evidences in one detector, but are unlikely to produce consistent signals in two or more observatories, implying  $\mathcal{Z}_{\text{incoherent}}$  is likely to dominate over  $\mathcal{Z}_{\text{coherent}}$ . Thus, astrophysical signals produce large BCR values while noise artefacts produce

small ones. This property has been leveraged to search, e.g., for intermediate mass black holes ([Vajpeyi et al. 2022](#)).

### 3. ANALYSIS

#### 3.1. *Injection and background studies*

We assess the significance of the BCR by performing 500 off-source searches at times around HLV GRB triggers with random sky locations. We discard times with significant data-quality issues. In Fig. 1 we plot the distribution of background BCR values in green.

Based on our background distribution, we determine that a value of  $\log_{10}(\text{BCR}) > 2.8$  is required in order to detect an event with  $p = 1/500$ . Accounting for trial factors, this corresponds to a  $p$ -value of

$$1 - (1 - 1/500)^{70} = 13\%, \quad (4)$$

given that we searched for 70 events. Thus, we do not expect any events with  $\log_{10}(\text{BCR}) > 2.8$  due to noise fluctuations. Glitches are expected to create a negative tail and there will likely be, by chance, some coherent data across detectors giving some positive values, which are seen in Fig. 1.

We verify our method by injecting binary neutron star merger signals into an off-source data segment with a three-detector network (i.e. HLV) and calculating the BCR. We vary the luminosity distance in order to see how the BCR depends on the network signal-to-noise ratio. The binary parameters for our injection are summarized in Table 2. For the sake of realism, we simulate the signal with a more accurate waveform template, IM-RPHENOMPv2\_NRTIDAL ([Dietrich et al. 2019](#)).

In Fig. 2 we plot  $\log_{10}(\text{BCR})$  versus network optimal SNR. The horizontal green line indicates the maximum off-source  $\log_{10}(\text{BCR})$  value from our background study. This shows we can identify a signal with a single-event (no trial factors)  $p$ -value of 0.2% with optimal network SNR  $\approx 8.5$  at a luminosity distance of 300 Mpc.

Additionally, we calculate the BCR of a recent HL sub-threshold binary neutron-star merger candidate GW231109\_235456 ([Niu et al. 2025](#)) and recover a  $\log_{10}(\text{BCR}) = 3.65$ , shown on Figures 1 and 2 in maroon, above the background thresholds shown in green. [Niu et al. \(2025\)](#) reports a network SNR of 9.7 using their search, which incorporates a redshift-corrected population model. Hypothetically<sup>4</sup>, if there had been a corresponding long GRB trigger, our BCR value would sug-

<sup>4</sup> Given there is no long GRB trigger, the background study we performed is not the one relevant to this event. Thus, we cannot comment beyond this hypothetical scenario as to the astrophysical nature of this candidate.

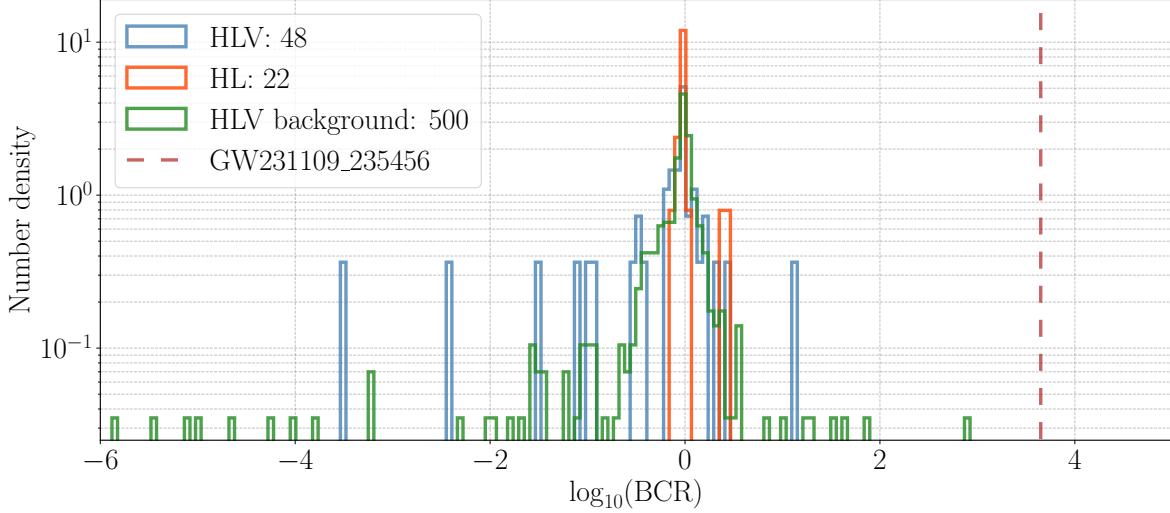


**Figure 1.** The distribution of Bayesian coherence ratio (BCR). The distribution for long GRBs coincident with HLV data is shown in blue, the distribution for long GRBs coincident with HL data is shown in orange, and the distribution of off-source data (with no long GRB trigger) is shown in green. The BCR of a recent HL sub-threshold binary neutron-star merger candidate GW231109\_235456 (Niu et al. 2025) is shown by the maroon vertical line.

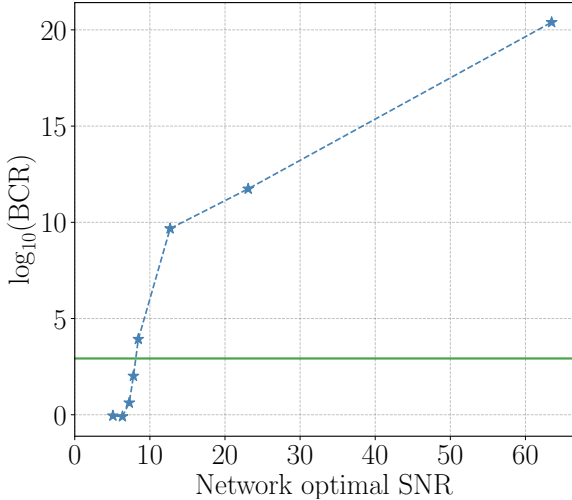


**Figure 2.** The Bayesian coherence ratio (blue) for a set of injected signals into a three-detector network (HLV) with varying luminosity distance, as described in Section 3.1. The background threshold, corresponding to the maximum off-source  $\log_{10}(\text{BCR}) = 2.8$  value, for a positive identification is shown in green. The BCR may provide evidence for sub-threshold events with network optimal  $\text{SNR} \approx 8 - 12$ .

Parameter	Value
$m_1$	$2.1 M_{\odot}$
$m_2$	$1.4 M_{\odot}$
$\chi_1$	0.01
$\chi_2$	0.01
$\Lambda_1$	600
$\Lambda_2$	600
$D_L$	[40, 110, 200, 300, 325, 350, 400, 500] Mpc
RA	1.215 rad
Dec	0.6086 rad
$\theta_{jn}$	0.679 rad
$\psi$	2.424 rad
$\phi_0$	2.198 rad
$t_0$	1260424370.938 s

**Table 2.** The parameters of the injected signal. Here,  $\chi_1, \chi_2$  are the spin magnitude of the primary and secondary objects, respectively,  $\theta_{jn}$  is the angle between the total angular momentum vector and line of sight,  $\psi$  is the polarisation angle,  $\phi$  is the binary phase at a given reference frequency,  $t_0$  is the geocentric coalescence time, and  $\Lambda_1, \Lambda_2$  are the tidal deformabilities of the primary and secondary objects, respectively.

gest the origin is astrophysical, and would be identified as a positive candidate for further investigation.<sup>5</sup>

### 3.2. Results and implications

In Fig. 1, we show our 48 HLV trigger BCR values in blue and 22 HL triggers in orange. These can be compared to our background BCR values shown in green, which shows that none of our triggers are louder than the largest background value. We conclude that we find no gravitational-wave counterparts. For individual BCR values for each GRB, see Appendix A.

We place an upper limit on the fraction of long gamma-ray bursts that are powered by binary mergers. This upper limit is somewhat model-dependent, and so we encourage the reader to treat it as a back-of-the-envelope calculation.

First, we write down the likelihood of observing  $N$  gravitationally bright long gamma-ray bursts given that a fraction  $f$  of long gamma ray bursts are gravitationally bright. The likelihood is a Poisson distribution

$$\mathcal{L}(N|f) = \frac{1}{N!} (fRVt_{\text{obs}})^N e^{-fRVt_{\text{obs}}}, \quad (5)$$

where  $V$  is the sensitive volume of the LVK network,  $R$  is the rate density of long gamma-ray bursts (units =  $\text{Gpc}^{-3} \text{yr}^{-1}$ ), and  $t_{\text{obs}}$  is the duration of the data set. This likelihood compares the *measured* number of gravitationally bright long GRBs with the *expected* number:

$$\hat{N} = fRVt_{\text{obs}}. \quad (6)$$

We assume the rate of electromagnetically-bright long GRBs detected by Fermi/Swift is  $R = 79^{+57}_{-33} \text{ Gpc}^{-3} \text{ yr}^{-1}$  (Ghirlanda & Salvaterra 2022). The typical jet opening angle associated with GRBs limits the number of long GRBs detected by Swift/Fermi, and so we apply a beaming correction factor  $f_b^{-1} = 260$  (corresponding to a jet opening angle of  $\approx 5^\circ$ ) (Wang et al. 2018; Ghirlanda et al. 2007; Liang et al. 2007).

We observe  $N = 0$  gravitationally bright long GRBs. We estimate the sensitive volume using posterior samples from our BILBY runs. In Sec. 3.1, we determine that a signal with network optimal SNR  $\sim 9$  would stand out above our background (with  $p = 17\%$  after trial factors).

<sup>5</sup> We perform a similar validation on GW170817, the first binary neutron star gravitational-wave signal, which had an associated short GRB. This was a three-detector (HLV) event with a network SNR of 32.4. The priors used in our analysis needed to be made stricter in order for the analysis to converge, and gave  $\log_{10}(\text{BCR}) \approx 10$ , broadly consistent with Fig. 2.

For the sake of convenience, we use this same SNR  $\sim 9$  to define our sensitive volume.<sup>6</sup>

For each event  $i$  we calculate  $\hat{d}_i$ : the comoving distance—averaged over 10 draws from our prior—with optimal SNR  $\rho_{\text{opt}} = 9$ :

$$\hat{d}_i = \int d\theta d_C(\theta) \pi(\theta) \Theta(\rho_{\text{opt}}^i > 9) \quad (7)$$

The variable  $\hat{d}_i$  is a measure of the “horizon” for which we can see binary systems drawn from our prior distribution. The horizon depends sensitively on our assumptions about the mass distribution of binaries powering long GRBs; more massive binaries can be detected further away. With that caveat, we calculate the sensitive volume given we are at low redshift:

$$V \approx \frac{4\pi}{3} \frac{1}{n} \sum_{i=1}^n (\hat{d}_i)^3. \quad (8)$$

We now have the ingredients to calculate the posterior for  $f$  (the fraction of gravitationally bright long GRBs):

$$p(f|N = 0) \propto e^{-fRV}. \quad (9)$$

The posterior for  $f$  is shown in Fig. 3. The solid blue curve marginalizes over uncertainty in the long GRB rate  $R$  while the shaded region shows how uncertainty in  $R$  affects our estimate of  $f$ . Given  $RV \approx 0.01$ , we find the posterior to be largely flat and uninformative, and predict  $f \lesssim 0.9$  with 90% credibility. The solid purple curve shows the same for  $RV \approx 4$ . This 500-fold increase in sensitive volume provides informative constraints and we find that  $f \lesssim 0.62$  with 90% credibility. This may not be achievable with current-generation gravitational-wave detectors, even with further upgrades.

The solid orange curve shows a similar calculation done assuming no associated gravitational waves are observed with the next-generation detector Cosmic Explorer (Evans et al. 2021), which will be sensitive to binary neutron star mergers up to redshift  $\sim 5$  (Evans et al. 2021). Here, we conservatively estimate the sensitive volume as  $1000 \text{ Gpc}^{-3}$ , and assume the long GRB rate increases by an order of magnitude between redshift 1 and 3. If thousands of long GRBs lie within the sensitive volume of Cosmic Explorer,  $f$  could be measured with high confidence.

Constraints on  $f$  under different assumptions remain largely uninformative without a substantial increase in sensitive volume. Even in the optimistic scenario

<sup>6</sup> This choice is somewhat arbitrary, but other parts of this calculation contribute more systematic uncertainty than any associated with our choice of threshold.

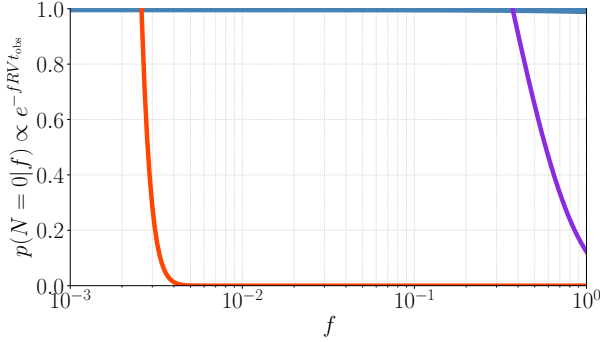


**Figure 3.** Estimated posterior distribution of  $f$ , the fraction of gravitationally-bright long GRBs originating from binary mergers. The blue curve shows constraints obtained using the current sensitive search volume, the purple curve assumes a 500-fold increase in sensitive volume, and the orange curve corresponds to a next-generation detector, Cosmic Explorer, under the assumption of no coincident long GRB and gravitational-wave detections, as described in Section 3.2. We can then constrain  $f$  to an upper limit of 0.90, 0.62, and 0.00 with 90% credibility, respectively. The shaded region plots the uncertainty from the rate of gravitationally-bright GRBs,  $R = 79^{+57}_{-33} \text{ Gpc}^{-3} \text{ yr}^{-1}$ .

where every successful jet launched by a binary neutron star merger produces a long GRB—corresponding to roughly one-fifth of the predicted merger rate of  $7.6 - 250 \text{ Gpc}^{-3} \text{ yr}^{-1}$ —predicted mergers (Salafia et al. 2022; Collaboration et al. 2025))—the expected event rate remains below the observed long-GRB rate. Assuming instead that all binary neutron star and neutron star–black hole mergers produce a successful long GRB only increases the rate by a factor of  $\sim 5$ . While these estimates are probabilistic, there remains a low but non-zero chance of observing a long GRB within the current sensitive search volume.

#### 4. CONCLUSION

Observations have long supported the bimodal distribution in the GRB population. Core-collapse supernovae have been associated with long GRBs based on sky localisation and spectra (Galama et al. 1998; Hjorth et al. 2003; Stanek et al. 2003; Hjorth & Bloom 2011). Kilonovae with short GRBs have been associated with compact binary mergers (Berger et al. 2013; Tanvir et al. 2013; Goldstein et al. 2017; Savchenko et al. 2017; Abbott et al. 2017b,a, 2019a). To date, the sole coincident GRB and gravitational-wave detection, GW170817 and GRB170817A, confirms binary neutron star mergers are a progenitor of some short GRBs and enabled significant multi-messenger campaigns, opening the door to a new frontier of science (Abbott et al. 2017b,c). However, this

picture has been challenged with evidence linking some long GRBs to binary mergers involving at least one neutron star.

We aim to fill a gap in the literature created by this new evidence, by performing a modelled search for sub-threshold binary mergers coincident with long GRBs. A confident detection of such an association would fundamentally reshape our understanding of GRB progenitors. We leverage the sky and time localisation provided by long GRBs to improve search sensitivity, and perform Bayesian inference on the data. We find no evidence for gravitational-wave signals coincident with long GRBs and set limits on the luminosity distance to each of these GRBs, assuming a neutron star or neutron star–black hole progenitor, ranging from 50 Mpc to 801 Mpc (90% credibility). We test our method on a sub-threshold binary-neutron star merger candidate, GW231109\_235456, with no GRB counterpart, not identified as a candidate via the conventional analysis priors. This method succeeds in identifying the hypothetical candidate with a  $\log_{10}(\text{BCR}) = 3.65$ , above the background threshold of  $\log_{10}(\text{BCR}) = 2.80$ .

We find that with the current sensitive search volume, we cannot place informative constraints on the fraction of long GRBs with binary merger associations. Using the rate of long GRBs in the local Universe, we estimate that at least a 500-fold increase in the sensitive search volume is required to begin constraining this fraction. There is still a non-zero chance we observe long GRBs within the sensitive volume. Future observing runs with improved detector sensitivity will increase the sensitive volume of our search, while the increased catalog of long GRBs will provide more opportunities for coincident detection. We plan to extend this targeted search approach to data from the fourth observing run of the LVK network, where these combined improvements will either enable the first detection of a gravitational-wave signal from a binary merger coincident with a long GRB, or further constrain the fraction of long GRBs originating from binary mergers involving a neutron star.

#### 5. ACKNOWLEDGMENTS

This research is supported by the Australian Research Council Centre of Excellence for Gravitational Wave Discovery (OzGrav), Project Numbers CE170100004 and CE230100016, Discovery Projects DP220101610 and DP230103088, and LIEF Project LE210100002. This material is based upon work supported by NSF’s LIGO Laboratory which is a major facility fully funded by the National Science Foundation. The authors are grateful for for computational resources provided by the LIGO Laboratory computing cluster at Cali-

fornia Institute of Technology supported by National Science Foundation Grants PHY-0757058 and PHY-0823459. This research has made use of the GRBSN webtool, available at <https://grbsn.watchertelescope.ie>,

and data from the Gravitational Wave Open Science Center (<https://www.gw-openscience.org>), a service of LIGO Laboratory, the LIGO Scientific Collaboration and the Virgo Collaboration.

## APPENDIX

### A. GRB DATA

We summarise the list of long GRBs used in this study in Table 3. These are the GRBs analysed by the LVK Collaboration when searching for collapsar signals (Abbott et al. 2021, 2022). We note the LVK GRB classification is based on the duration over which the fluence of the signal in the relevant GRB detector increases from 5% to 95%, denoted  $T_{90}$ , with associated error,  $\delta T_{90}$  (Abbott et al. 2021, 2022). There are therefore minor differences in reported  $T_{90}$  between detectors (i.e., between Swift and Fermi). The LVK Collaboration sorts GRBs into three categories,

$$\text{Class}(T_{90}, \delta T_{90}) = \begin{cases} \text{short}, & T_{90} + |\delta T_{90}| < 2 \text{ s}, \\ \text{long}, & T_{90} - |\delta T_{90}| > 4 \text{ s}, \\ \text{ambiguous}, & \text{otherwise.} \end{cases}$$

A more stringent classification would include spectral information and burst energetics.

In Table 3, we quote the LVK detector network used for the analysis (HL—LIGO Hanford and LIGO Livingston, HLV—LIGO Hanford, LIGO Livingston, and Virgo),  $\log_{10}(\text{BCR})$ , and  $D_{90}$ —the 90% lower credible bound on  $D_L$  posteriors. The  $D_L$  posteriors are a measure of the detector sensitivity at that time and sky localisation given we do not observe a merger. Thus, we can set limits on the luminosity distance to each of these long GRBs under the assumption that they were powered by a binary merger ranging from 50 Mpc to 801 Mpc.

## REFERENCES

Aasi, J., e. a. 2014, Physical Review Letters, 113, doi: [10.1103/physrevlett.113.011102](https://doi.org/10.1103/physrevlett.113.011102)

Aasi, J., et al. 2015, Classical and Quantum Gravity, 32, 074001, doi: [10.1088/0264-9381/32/7/074001](https://doi.org/10.1088/0264-9381/32/7/074001)

Abbott, B., Abbott, R., Abbott, T., et al. 2017a, Physical Review Letters, 119, doi: [10.1103/physrevlett.119.161101](https://doi.org/10.1103/physrevlett.119.161101)

—. 2019a, Physical Review X, 9, doi: [10.1103/physrevx.9.011001](https://doi.org/10.1103/physrevx.9.011001)

Abbott, B. P., Abbott, R., Abbott, T. D., et al. 2017b, The Astrophysical Journal Letters, 848, L13, doi: [10.3847/2041-8213/aa920c](https://doi.org/10.3847/2041-8213/aa920c)

—. 2017c, The Astrophysical Journal Letters, 848, L12, doi: [10.3847/2041-8213/aa91c9](https://doi.org/10.3847/2041-8213/aa91c9)

—. 2019b, The Astrophysical Journal, 886, 75, doi: [10.3847/1538-4357/ab4b48](https://doi.org/10.3847/1538-4357/ab4b48)

Abbott, B. P., e. a. 2017, The Astrophysical Journal, 841, 89, doi: [10.3847/1538-4357/aa6c47](https://doi.org/10.3847/1538-4357/aa6c47)

Abbott, R., Abbott, T. D., Acernese, F., et al. 2022, The Astrophysical Journal, 928, 186, doi: [10.3847/1538-4357/ac532b](https://doi.org/10.3847/1538-4357/ac532b)

Abbott, R., Abe, H., Acernese, F., et al. 2023a, The Astrophysical Journal Supplement Series, 267, 29, doi: [10.3847/1538-4365/acdc9f](https://doi.org/10.3847/1538-4365/acdc9f)

Abbott, R., Abbott, T. D., Abraham, S., et al. 2021, The Astrophysical Journal, 915, 86, doi: [10.3847/1538-4357/abee15](https://doi.org/10.3847/1538-4357/abee15)

Abbott, R., Abbott, T., Acernese, F., et al. 2023b, Physical Review X, 13, doi: [10.1103/physrevx.13.041039](https://doi.org/10.1103/physrevx.13.041039)

Acernese, F., et al. 2014, Classical and Quantum Gravity, 32, 024001, doi: [10.1088/0264-9381/32/2/024001](https://doi.org/10.1088/0264-9381/32/2/024001)

Akutsu, T., et al. 2020, Overview of KAGRA: Detector design and construction history. <https://arxiv.org/abs/2005.05574>

Ashton, G., & Thrane, E. 2020, Mon. Not. R. Ast. Soc., 498, 1905

Ashton, G., Thrane, E., & R. J. E. Smith. 2019a, Phys. Rev. D, 100, 123018

Ashton, G., et al. 2019b, Astrophys. J. Suppl., 241, 27, doi: [10.3847/1538-4365/ab06fc](https://doi.org/10.3847/1538-4365/ab06fc)

Barthelmy, S. D., Barbier, L. M., Cummings, J. R., et al. 2005, SSRv, 120, 143, doi: [10.1007/s11214-005-5096-3](https://doi.org/10.1007/s11214-005-5096-3)

GRB Name	Network	$\log_{10}(\text{BCR})$	$D_{90}$ (Mpc)	GRB Name	Network	$\log_{10}(\text{BCR})$	$D_{90}$ (Mpc)
GRB190404293	HLV	-0.19	175	GRB190926A	HL	-0.12	294
GRB190406450	HLV	-3.49	51	GRB191110A	HLV	-0.47	324
GRB190504415	HLV	-0.02	498	GRB191111A	HL	-0.04	612
GRB190507270	HL	-0.09	187	GRB191119261	HL	0.01	700
GRB190507970	HLV	-0.07	608	GRB191122A	HLV	-0.07	289
GRB190511A	HLV	-0.52	287	GRB191125A	HLV	1.13	273
GRB190512A	HLV	-0.12	458	GRB191202A	HLV	-0.42	241
GRB190519A	HLV	0.21	394	GRB191225B	HL	0.01	683
GRB190603795	HLV	0.00	702	GRB200105914	HLV	0.10	150
GRB190604446	HL	0.37	472	GRB200112395	HLV	0.10	152
GRB190612165	HLV	-0.04	801	GRB200112A	HLV	-0.02	639
GRB190613A	HLV	-0.97	462	GRB200114A	HLV	0.01	630
GRB190613B	HL	-0.05	595	GRB200115A	HL	0.00	492
GRB190615636	HLV	-9.89	50	GRB200122A	HLV	0.01	349
GRB190620507	HL	0.00	671	GRB200125B	HL	0.02	467
GRB190628521	HL	-0.03	411	GRB200127B	HL	0.45	169
GRB190630C	HLV	-1.50	219	GRB200130B	HL	0.00	702
GRB190701A	HLV	-2.40	110	GRB200131A	HLV	-0.04	371
GRB190707308	HL	-0.03	303	GRB200201A	HLV	-0.02	262
GRB190712095	HLV	-0.20	481	GRB200205C	HL	-0.09	308
GRB190718A	HL	-0.03	562	GRB200211A	HL	-0.02	575
GRB190719499	HLV	-0.05	289	GRB200212A	HL	-0.05	579
GRB190720613	HLV	0.00	620	GRB200216B	HLV	0.21	184
GRB190720964	HL	0.00	711	GRB200219A	HLV	0.31	413
GRB190726642	HLV	0.02	249	GRB200219B	HLV	-0.01	374
GRB190726843	HLV	0.45	322	GRB200224B	HLV	0.08	186
GRB190805106	HLV	-0.21	349	GRB200227A	HLV	0.00	547
GRB190805199	HLV	-0.06	154	GRB200301320	HLV	-0.48	590
GRB190806535	HLV	-0.16	281	GRB200303A	HLV	0.05	273
GRB190824A	HL	-0.07	593	GRB200308A	HLV	-0.93	248
GRB190827467	HL	0.00	745	GRB200313A	HLV	-0.16	418
GRB190831693	HLV	-1.09	183	GRB200317A	HLV	0.00	795
GRB190906767	HLV	-0.15	325	GRB200319A	HL	-0.03	739
GRB190910028	HLV	-33.82	50	GRB200320A	HLV	-0.01	371
GRB190916590	HLV	0.13	381	GRB200326A	HLV	-0.07	302

**Table 3.** Long GRBs detected by Swift and Fermi that were followed up in our analysis. We report the  $\log_{10}(\text{BCR})$  and  $D_{90}$ —the lower 90% credible limit on the  $D_L$  posterior.

Berger, E., Fong, W., & Chornock, R. 2013, The Astrophysical Journal, 774, L23, doi: [10.1088/2041-8205/774/2/l23](https://doi.org/10.1088/2041-8205/774/2/l23)

Berlato, F., Greiner, J., & Burgess, J. M. 2019, The Astrophysical Journal, 873, 60, doi: [10.3847/1538-4357/ab0413](https://doi.org/10.3847/1538-4357/ab0413)

Collaboration, T. L. S., the Virgo Collaboration, & the KAGRA Collaboration, e. a. 2025, GWTC-4.0: Population Properties of Merging Compact Binaries. <https://arxiv.org/abs/2508.18083>

Della Valle, M., Chincarini, G., Panagia, N., et al. 2006, Nature, 444, 1050, doi: [10.1038/nature05374](https://doi.org/10.1038/nature05374)

Dietrich, T., Samajdar, A., Khan, S., et al. 2019, Physical Review D, 100, doi: [10.1103/physrevd.100.044003](https://doi.org/10.1103/physrevd.100.044003)

Eichler, D., Livio, M., Piran, T., & Schramm, D. N. 1989, Nature, 340, 126, doi: [10.1038/340126a0](https://doi.org/10.1038/340126a0)

Evans, M., Adhikari, R. X., Afle, C., et al. 2021, A Horizon Study for Cosmic Explorer: Science, Observatories, and Community. <https://arxiv.org/abs/2109.09882>

Finneran, G., Cotter, L., & Martin-Carrillo, A. 2025, *Astronomy and Computing*, 52, 100954, doi: [10.1016/j.ascom.2025.100954](https://doi.org/10.1016/j.ascom.2025.100954)

Galama, T. J., Vreeswijk, P. M., van Paradijs, J., et al. 1998, *Nature*, 395, 670, doi: [10.1038/27150](https://doi.org/10.1038/27150)

Gehrels, N., Chincarini, G., Giommi, P., et al. 2004, *ApJ*, 611, 1005, doi: [10.1086/422091](https://doi.org/10.1086/422091)

Gehrels, N., Norris, J. P., Barthelmy, S. D., et al. 2006, *Nature*, 444, 1044, doi: [10.1038/nature05376](https://doi.org/10.1038/nature05376)

Ghirlanda, G., Nava, L., Ghisellini, G., & Firmani, C. 2007, *A&A*, 466, 127, doi: [10.1051/0004-6361:20077119](https://doi.org/10.1051/0004-6361:20077119)

Ghirlanda, G., & Salvaterra, R. 2022, The Cosmic History of Long Gamma Ray Bursts. <https://arxiv.org/abs/2206.06390>

Gillanders, J. H., & Smartt, S. J. 2025, Analysis of the JWST spectra of the kilonova AT 2023vfi accompanying GRB 230307A. <https://arxiv.org/abs/2408.11093>

Goldstein, A., Veres, P., Burns, E., et al. 2017, *ApJL*, 848, L14, doi: [10.3847/2041-8213/aa8f41](https://doi.org/10.3847/2041-8213/aa8f41)

Gompertz, B. P., Ravasio, M. E., Nicholl, M., et al. 2022, *Nature Astronomy*, 7, 67–79, doi: [10.1038/s41550-022-01819-4](https://doi.org/10.1038/s41550-022-01819-4)

Gottlieb, O., Metzger, B., Quataert, E., et al. 2023, A Unified Picture of Short and Long Gamma-ray Bursts from Compact Binary Mergers. <https://arxiv.org/abs/2309.00038>

Harry, I. W., & Fairhurst, S. 2011, *Physical Review D*, 83, doi: [10.1103/physrevd.83.084002](https://doi.org/10.1103/physrevd.83.084002)

Hjorth, J., & Bloom, J. S. 2011, The Gamma-Ray Burst - Supernova Connection. <https://arxiv.org/abs/1104.2274>

Hjorth, J., Sollerman, J., Møller, P., et al. 2003, *Nature*, 423, 847, doi: [10.1038/nature01750](https://doi.org/10.1038/nature01750)

Husa, S., Khan, S., Hannam, M., et al. 2016, *Physical Review D*, 93, doi: [10.1103/physrevd.93.044006](https://doi.org/10.1103/physrevd.93.044006)

Isi, M., Smith, R., Vitale, S., et al. 2018, *Physical Review D*, 98, doi: [10.1103/physrevd.98.042007](https://doi.org/10.1103/physrevd.98.042007)

Jin, Z.-P., Li, X., Cano, Z., et al. 2015, *The Astrophysical Journal*, 811, L22, doi: [10.1088/2041-8205/811/2/l22](https://doi.org/10.1088/2041-8205/811/2/l22)

Khan, S., Husa, S., Hannam, M., et al. 2016, *Physical Review D*, 93, doi: [10.1103/physrevd.93.044007](https://doi.org/10.1103/physrevd.93.044007)

Kouveliotou, C., Meegan, C. A., Fishman, G. J., et al. 1993, *ApJL*, 413, L101, doi: [10.1086/186969](https://doi.org/10.1086/186969)

Kyutoku, K., Shibata, M., & Taniguchi, K. 2021, *Living Reviews in Relativity*, 24, doi: [10.1007/s41114-021-00033-4](https://doi.org/10.1007/s41114-021-00033-4)

Levan, A. J., Gompertz, B. P., Salafia, O. S., et al. 2023, *Nature*, 626, 737–741, doi: [10.1038/s41586-023-06759-1](https://doi.org/10.1038/s41586-023-06759-1)

Liang, E., Zhang, B., Virgili, F., & Dai, Z. G. 2007, *The Astrophysical Journal*, 662, 1111–1118, doi: [10.1086/517959](https://doi.org/10.1086/517959)

Maccary, R., Guidorzi, C., Maistrello, M., et al. 2026, *Journal of High Energy Astrophysics*, 49, 100456, doi: [10.1016/j.jheap.2025.100456](https://doi.org/10.1016/j.jheap.2025.100456)

Meegan, C., Lichti, G., Bhat, P. N., et al. 2009, *ApJ*, 702, 791, doi: [10.1088/0004-637X/702/1/791](https://doi.org/10.1088/0004-637X/702/1/791)

Narayan, R., Paczynski, B., & Piran, T. 1992, *The Astrophysical Journal*, 395, L83, doi: [10.1086/186493](https://doi.org/10.1086/186493)

Neights, E., Burns, E., Fryer, C. L., et al. 2025, *Monthly Notices of the Royal Astronomical Society*, 545, doi: [10.1093/mnras/staf2019](https://doi.org/10.1093/mnras/staf2019)

Niu, W., Hanna, C., Haster, C.-J., et al. 2025, GW231109\_235456: A Sub-threshold Binary Neutron Star Merger in the LIGO-Virgo-KAGRA O4a Observing Run? <https://arxiv.org/abs/2509.09741>

Paczynski, B. 1991, *AcA*, 41, 257

Paczynski, B. 1998, *The Astrophysical Journal*, 494, L45–L48, doi: [10.1086/311148](https://doi.org/10.1086/311148)

Popham, R., Woosley, S. E., & Fryer, C. 1999, *The Astrophysical Journal*, 518, 356–374, doi: [10.1086/307259](https://doi.org/10.1086/307259)

Rastinejad, J. C., Gompertz, B. P., Levan, A. J., et al. 2022, *Nature*, 612, 223–227, doi: [10.1038/s41586-022-05390-w](https://doi.org/10.1038/s41586-022-05390-w)

Romero-Shaw, I. M., et al. 2020, *Mon. Not. Roy. Astron. Soc.*, 499, 3295, doi: [10.1093/mnras/staa2850](https://doi.org/10.1093/mnras/staa2850)

Rosswog, S., Diener, P., Torsello, F., Tauris, T. M., & Sarin, N. 2024, Mergers of double neutron stars with one high-spin component: brighter kilonovae and fallback accretion, weaker gravitational waves. <https://arxiv.org/abs/2310.15920>

Salafia, O. S., Colombo, A., Gabrielli, F., & Mandel, I. 2022, *Astronomy & Astrophysics*, 666, A174, doi: [10.1051/0004-6361/202243260](https://doi.org/10.1051/0004-6361/202243260)

Sathyaprakash, B. S., & Schutz, B. F. 2009, *Living Reviews in Relativity*, 12, doi: [10.12942/lrr-2009-2](https://doi.org/10.12942/lrr-2009-2)

Savchenko, V., Ferrigno, C., Kuulkers, E., et al. 2017, *ApJL*, 848, L15, doi: [10.3847/2041-8213/aa8f94](https://doi.org/10.3847/2041-8213/aa8f94)

Shibata, M., & Uryū, K. 2006, *Physical Review D*, 74, doi: [10.1103/physrevd.74.121503](https://doi.org/10.1103/physrevd.74.121503)

Stanek, K. Z., Matheson, T., Garnavich, P. M., et al. 2003, *ApJL*, 591, L17, doi: [10.1086/376976](https://doi.org/10.1086/376976)

Sun, H., Wang, C. W., Yang, J., et al. 2024, Magnetar emergence in a peculiar gamma-ray burst from a compact star merger. <https://arxiv.org/abs/2307.05689>

Sutton, P. J., Jones, G., Chatterji, S., et al. 2010, *New Journal of Physics*, 12, 053034, doi: [10.1088/1367-2630/12/5/053034](https://doi.org/10.1088/1367-2630/12/5/053034)

Tanvir, N. R., Levan, A. J., Fruchter, A. S., et al. 2013, *Nature*, 500, 547–549, doi: [10.1038/nature12505](https://doi.org/10.1038/nature12505)

Tohuvavohu, A., Kennea, J. A., DeLaunay, J., et al. 2020, *The Astrophysical Journal*, 900, 35, doi: [10.3847/1538-4357/aba94f](https://doi.org/10.3847/1538-4357/aba94f)

Troja, E., Fryer, C. L., O'Connor, B., et al. 2022, *Nature*, 612, 228, doi: [10.1038/s41586-022-05327-3](https://doi.org/10.1038/s41586-022-05327-3)

Vajpeyi, A., Smith, R., Thrane, E., et al. 2022, *Mon. Not. R. Ast. Soc.*, 516, 5309

Veitch, J., & Vecchio, A. 2010, *Physical Review D*, 81, 062003, doi: [10.1103/PhysRevD.81.062003](https://doi.org/10.1103/PhysRevD.81.062003)

Wang, X.-G., Zhang, B., Liang, E.-W., et al. 2018, *ApJ*, 859, 160, doi: [10.3847/1538-4357/aabc13](https://doi.org/10.3847/1538-4357/aabc13)

Wang, Y.-F., Nitz, A. H., Capano, C. D., et al. 2022, *The Astrophysical Journal Letters*, 939, L14, doi: [10.3847/2041-8213/ac990c](https://doi.org/10.3847/2041-8213/ac990c)

Williamson, A., Biwer, C., Fairhurst, S., et al. 2014, *Physical Review D*, 90, doi: [10.1103/physrevd.90.122004](https://doi.org/10.1103/physrevd.90.122004)

Woosley, S. E. 1993, *ApJ*, 405, 273, doi: [10.1086/172359](https://doi.org/10.1086/172359)

Was, M., Sutton, P. J., Jones, G., & Leonor, I. 2012, *Physical Review D*, 86, doi: [10.1103/physrevd.86.022003](https://doi.org/10.1103/physrevd.86.022003)

Yang, J., Ai, S., Zhang, B.-B., et al. 2022, *Nature*, 612, 232–235, doi: [10.1038/s41586-022-05403-8](https://doi.org/10.1038/s41586-022-05403-8)

Yang, Y.-H., Troja, E., O'Connor, B., et al. 2023, A lanthanide-rich kilonova in the aftermath of a long gamma-ray burst. <https://arxiv.org/abs/2308.00638>

Yi, S.-X., Yorgancioglu, E. S., Xiong, S. L., & Zhang, S. N. 2025, Long Pulse by Short Central Engine: Prompt emission from expanding dissipation rings in the jet front of gamma-ray bursts. <https://arxiv.org/abs/2411.16174>

Zhang, B. 2018, *The Physics of Gamma-Ray Bursts* (Cambridge University Press), doi: [10.1017/9781139226530](https://doi.org/10.1017/9781139226530)

Zhang, B., Zhang, B.-B., Liang, E.-W., et al. 2007, *The Astrophysical Journal*, 655, L25–L28, doi: [10.1086/511781](https://doi.org/10.1086/511781)

Zhang, H.-M., Huang, Y.-Y., Zheng, J.-H., Liu, R.-Y., & Wang, X.-Y. 2022, *ApJL*, 933, L22, doi: [10.3847/2041-8213/ac7b23](https://doi.org/10.3847/2041-8213/ac7b23)

Zhu, S.-Y., Deng, H.-Y., Zhang, F.-W., Mo, Q.-Z., & Tam, P.-H. T. 2025, Identifying Merger-Driven Long Gamma-Ray Bursts based on Machine Learning. <https://arxiv.org/abs/2506.08675>